Measuring ice shelf draft and seabed topography below Fimbulisen

Ole Anders Nøst
Norwegian Polar Institute,
Polar Environmental Center, Tromsø, Norway

1 Introduction

Along the Dronning Maud Land coast the westward flowing coastal current brings relatively fresh and cold surface water westward into the southern Weddell Sea (Gill 1973; Whitworth et al. 1998). Along its path the coastal current is modified by coastal polynyas (Markus et al. 1998) and interactions with the ice shelves. Due to the narrow continental shelves the ice shelves come into close proximity with the Warm Deep Water, and this may lead to high melt rates and freshwater input to the ocean (Fahrbach et al. 1994). Grosfeld et al. (1995, 1997) showed that the exchange across the ice shelf front occurred in regions where contours of constant water column thickness crossed the ice front. Therefore, to understand the complicated processes along the Antarctic Coast it is crucial to know the topography beneath the ice shelves.

Along the Dronning Maud Land coast the seabed beneath the ice shelves are largely unknown. In the 2000/2001 season a group from the Norwegian Polar Institute mapped the seabed topography and ice shelf thickness on the Fimbulisen ice shelf. In this report results from seismic reflection and refraction surveys on Fimbulisen are presented.

2 Study area

The continental shelf along the Dronning Maud Land coast is narrow, in the order of 10 km from the ice shelf front to the continental shelf break (see figure 1). Some places the ice shelf covers the whole continental shelf and the ice shelf front is located above the continental slope. The depth of the continental shelf varies from about 200 m to about 6-700 m. At the continental shelf break the depth increases rapidly to about 4000 meter. Fimbulisen is an ice shelf located at the Dronning Maud Land coast (Figure 1). Fimbulisen is divided into three distinct regions, a western and eastern part of flat-lying ice shelf delineated by ice rises and a central part located between extensively crevassed zones. The crevasse zones are caused as Jutulstraumen ice stream forces its way through Fimbulisen. The central part is about 20 km wide at the grounding line and about 100 km wide at the coast.

Our route on Fimbulisen in the 2000/01 field season is shown in Figure 2. As shown we have covered most of Fimbulisen, except for the southermost part of Jutulstraumen and the crevassed zones on both sides of Jutulstraumen.

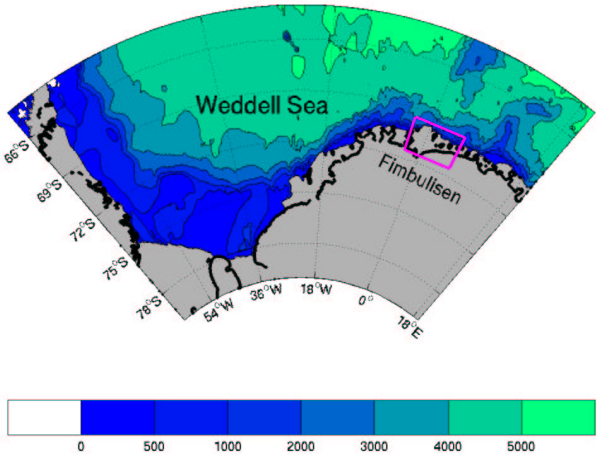

Figure 1: Sea-bed topography of the Weddell Sea. The location of Fimbulisen on the Dronning Maud Land coast is shown.

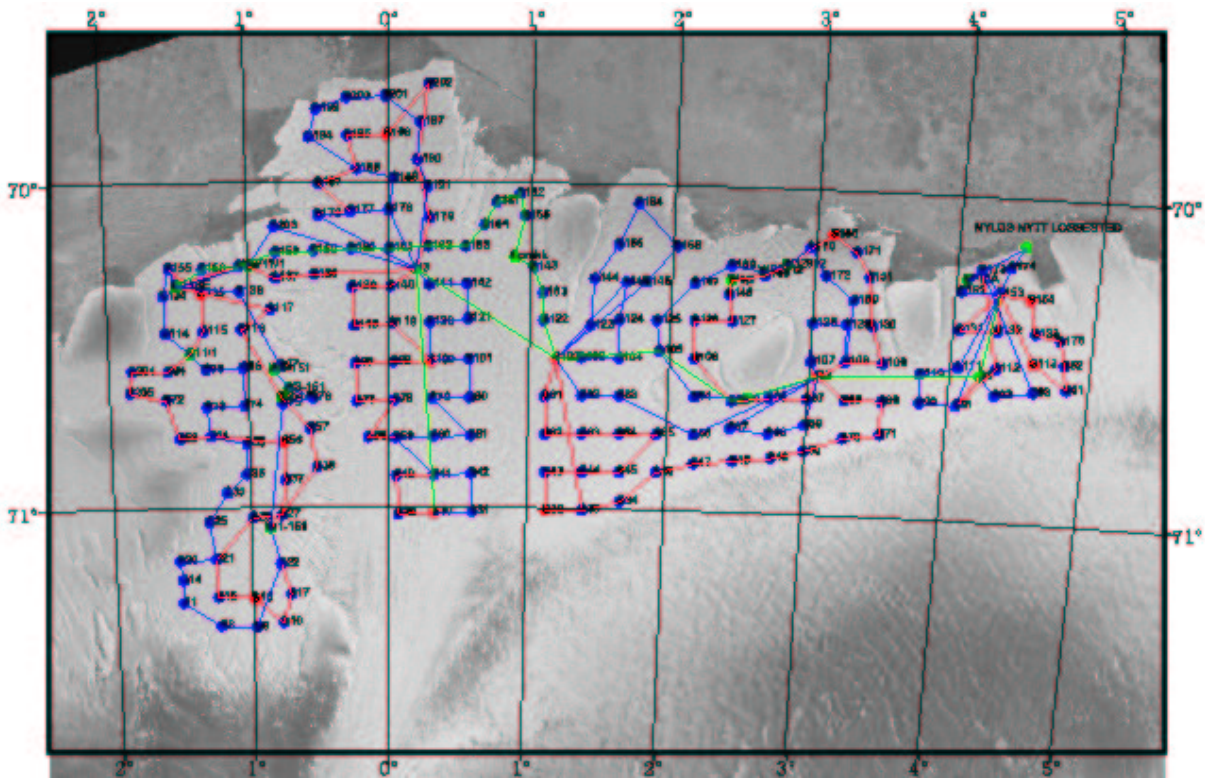

Figure 2: A Radarsat image of Fimbulisen with stations and routes. Reflection measurements are marked with blue points, refraction measurements by red points, and green points are waypoints on the route with no measurements. The red and blue lines are the routes of the two teams, while the green route is where the two teams travelled together.

3 Measurements

3.1 Reflection surveys

To be able to cover the entire ice shelf we divided into two teams, both equipped with a 24 channel ABEM Terraloc Mark 6 seismograph. At each station a 4 m deep shot hole was drilled. The holes were charged with 300-600 g of explosives and filled back with snow. The shots were detected by 24 vertically oriented geophones at offsets between 10 and 240 m from the source. The geophones were planted at a depth of about 0.4 m to ensure a firm coupling with the snow and for protection from wind noise. The sample interval was 0.25 ms. These reflection measurements were conducted at a total of 183 points, all shown in Figure 2. An example of a reflection record is shown in Figure 3.

The reflections from the ice base and from the seabed were in most cases easy to identify. However, in some regions near the grounding lines or the crevassed zones on both sides of Jutulstraumen, the reflections were weaker and in some cases impossible to identify. These stations are all near the crevasse zones on both sides of Jutulstraumen, and therefore, we believe that the weak reflections are caused by crevasses or smaller cracks which influences the sound wave, even if no signs of crevasses were seen on the surface.

3.2 Refraction surveys

In order to calculate ice thickness from the reflection data the seismic velocity in the ice has to be known. In the upper 80-100 m the density of the snow and firn, and thereby also the seismic velocity, increases with depth. In order to calculate the velocity profile in this upper layer we conducted 12 shallow refraction surveys distributed as shown in Figure 2.

In the refraction surveys we used 48 geophones at offsets between 1 and 384 m (Table 1). To do this we used two shots as we only had a 24 channel seismograph. Sample interval was 0.1 ms. The charge for shot 1 was 2 detonators and for shot 2 it was 60 g of explosives. Shot depth for shot 2 was 1 meter while it was about 40 cm for shot 1. All geophones were planted at a depth of about 40 cm.

Table 1

Shot no.	Geophone distance (meter)
1	1, 2.5, 5, 7.5, 10, 12.5, 15, 20, 25, 30, 35, 40, 45, 50, 60, ..., 150
2	154, 164, 174, 184, 194, 204, ...384

4 Analysis of data and results

4.1 Refraction surveys

To convert the time-distance data of the first arrivals to velocity depth profiles, we assume that there are no horizontal variations and that the velocity is monotonically increasing with depth. The calculated velocities from the 12 different refraction surveys are shown in Figure 4. The uncertainty in the velocity calculated is about 100 m/s for the profile calculated at S154, but it is up to 300 m/s for the profiles calculated at S30 and S32 near crevasse zones. These two profiles are the ones with highest velocity seen in Figure 4.

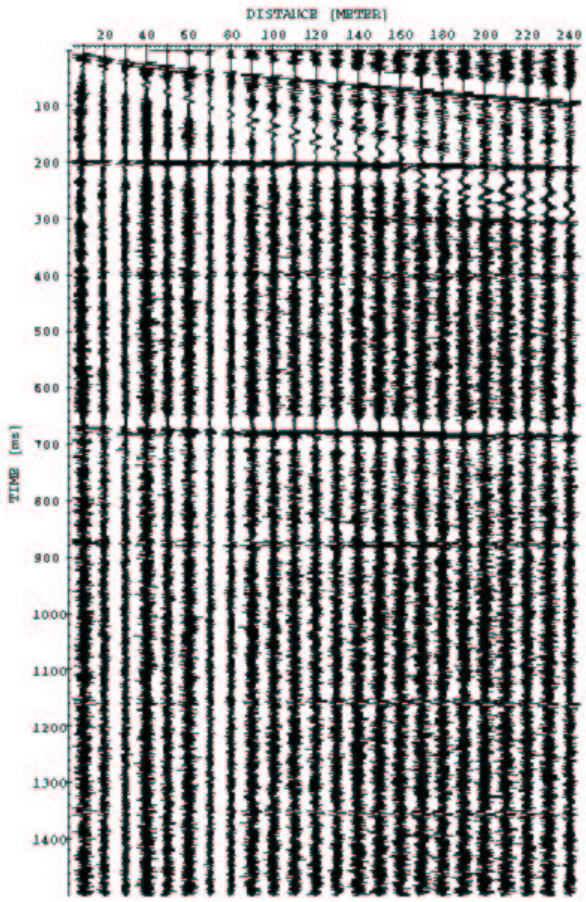

Figure 3: The seismic record from the reflection measurement at S154. The reflection from the base of the ice is seen near 200 ms, and the reflection from the seabed is seen near 670 ms. The other reflections seen is multiples.

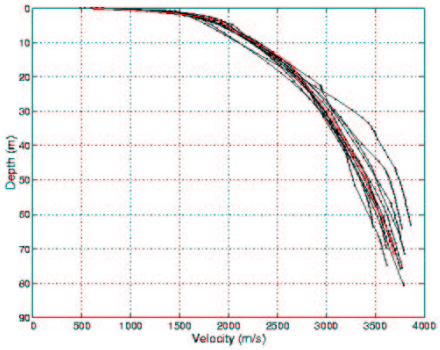

Figure 4: The velocity profiles calculated from the refraction data. The red curve is the velocity profile at S154.

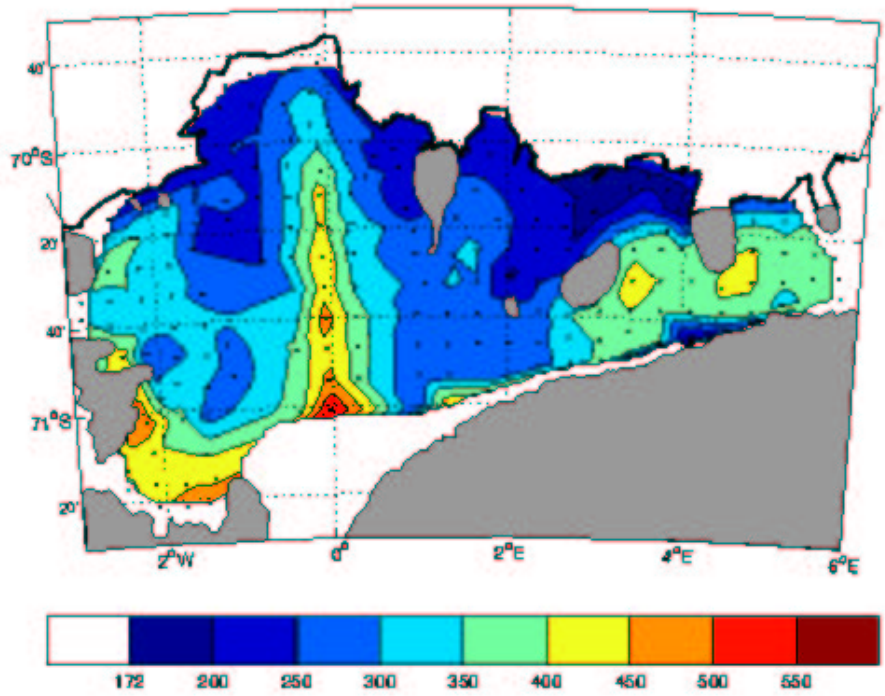

Figure 5: Ice thickness distribution. Black dots are the position of the measurements.

4.2 Reflection surveys

For the velocity in the upper 100 m we use the average velocity of the profile calculated from the refraction data at S154, setting the velocity at 100 m to 3800 m/s. The mean velocity for the upper 100 m is then 3017 m/s. From 100 m depth to the ice shelf draft we set the velocity to 3810 m/s, which is similar to the sound velocity used in seismic measurements on Ronne (Smith and Doake 1994; Johnson and Smith 1997) and Ross (Robertson and Bentley 1990) Ice Shelves. The sound velocity in the ocean below the ice shelf is set to 1450 m/s.

4.3 Ice and water column thickness distributions

The ice thickness and water column thickness may now be obtained from the measured travel times. The ice thickness distribution is shown in Figure 5 and the water column thickness in Figure 6. A rough analysis of the accuracy suggests that the ice thickness is within 5m, and the water column thickness is within 10m. The ice thickness varies from about 170 m to more than 500 m in the Jutulstraumen area. The water column thickness is more than 900 m in the central part of the ice shelf. At the northernmost area of Fimbulisen the ice shelf is located above the continental slope. If one assumes that the ocean currents follow contours of constant water column thickness there will be a significant exchange between the ice shelf cavity and the open ocean, and the currents will reach the areas close to the grounding line.

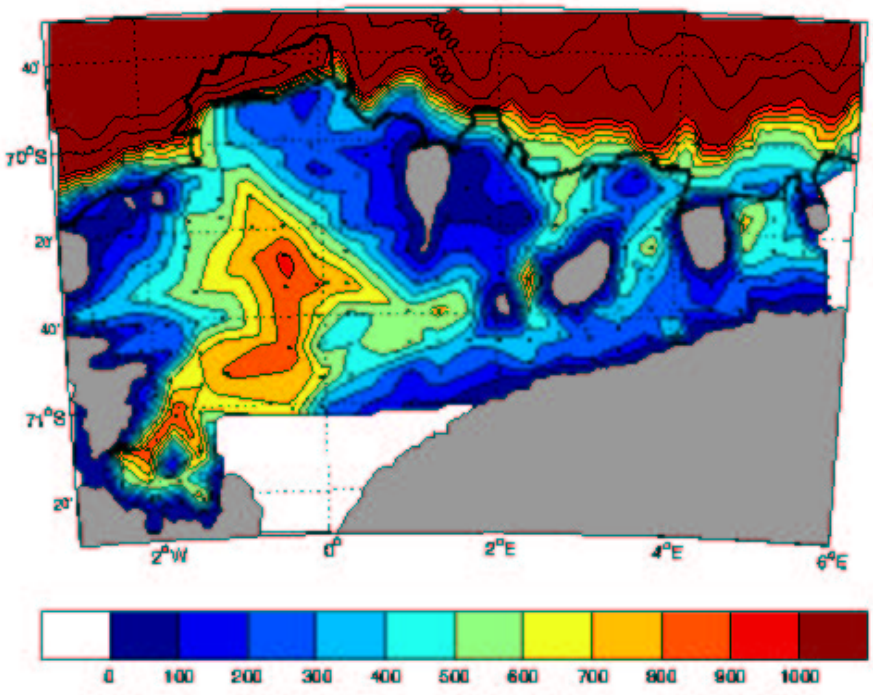

Figure 6: Water column thickness distribution. Black dots are the position of the measurements.

Acknowledgements. Thanks to Harvey Goodwin, Tore Rnstad and Stein Hugo Thorsen for invaluable help during the field work, and to Andy Smith and Mark Johnson for help and advise during the preparation of the field work. This work was sponsored by the Norwegian Research Council.

References

Fahrbach, E., R. G. Peterson, G. Rohardt, P. Schlosser, and R. Bayer 1994. Suppression of bottom water formation in the south-eastern Weddell Sea. *Deep Sea Res.*, Vol 41, pp. 389–411.

Gill, A. E. 1973. Circulation and bottom water formation in the Weddell Sea. *Deep Sea Res.*, Vol 20, pp. 111–140.

Grosfeld, K., J. Determann, and R. Gerde 1995. Interaction between ice shelf cavities and the open ocea. In H. Oerter (Ed.), *Filchner Ronne Ice Shelf programme, report no. 9*, Alfred Wegener Institute, Bremerhaven, pp. 23–30.

Grosfeld, K., R. Gerdes, and J. Determann 1997. Thermohaline circulation and the interaction between ice shelf cavities and the adjacent open ocean. *J. Geophys. Res.*, Vol 102, pp. 15595–15610.

Johnson, M. R. and A. M. Smith 1997. Seabed topography under the southern and western Ronne Ice Shelf, derived from seismic surveys. *Ant. Science. 9*(2), pp. 201–208.

Markus, T., C. Kottmeier, and E. Fahrbach 1998. Ice formation in coastal polynyas in the Weddell Sea and their impact on oceanic salinity. In M. JEFFRIES (Ed.), *Antarctic sea ice: Physical processes, interaction and variability*, Volume 74 of *Antarctic Research Series*, pp. 273–292. American Geophysical Union.

Robertson, J. D. and C. R. Bentley 1990. Seismic studies on the grid western half of the Ross Ice Shelf: RIGGS I and RIGGS II. In C. R. BENTLEY AND D. E. HAYES (Eds.), *The Ross Ice Shelf: Glaciology and geophysics*, Volume 42 of *Antarctic Research Series*, pp. 55–86. American Geophysical Union.

Smith, A. M. and C. S. M. Doake 1994. Sea-bed depths at the mouth of Rutford Ice Stream, Antarctica. *Annals of Glaciology*, Vol 20, pp. 353–356.

Whitworth, T., A. H. Orsi, S. J. Kim, W. D. Nowlin, and R. A. Locarnini 1998. Water masses and mixing near the Antarctic Slope Front. In S. S. JACOBS AND R. F. WEISS (Eds.), *Ocean, ice and atmosphere: Interactions at the Antarctic continental margin*, Volume 75 of *Antarctic Research Series*, pp. 1–27. American Geophysical Union.